

UNIFIED CONTROL OF DC-DC CONVERTERS USING GAIN SCHEDULED DYNAMIC ADAPTIVE CONTROLLER FOR PORTABLE DEVICE APPLICATIONS

K.Kanimozhi

ULTRA College of Engineering and Technology for Women,
Madurai, Tamil Nadu , India, kanillaith2003@gmail.com

B.Raja Mohamed Rabi

ULTRA College of Engineering and Technology for Women,
Madurai, Tamil Nadu , India, rabime2002@yhao.co.in

Abstract: *The problem considered in this paper is improving the dynamic response of DC-DC converter system with internal parameter uncertainties. The methodology of sliding mode control in existing works is based on Proportional Integral and Derivative Controller (PID). The present work addresses various issues on a unified approach for design and application of pulse-width modulation (PWM) based Digital Adaptive Sliding Mode (ASM) equivalent control technique to buck converter for mobile phones operating in continuous conduction mode (CCM) and discontinuous conduction mode (DCM). The controller is gain scheduled to monitor the output loading condition, and adaptively changes the control parameters to give optimal dynamic performance corresponding to any load variations. Further stability is analytically verified using Lyapunov stability criterion and system is proved to be globally asymptotically stable. Finally effectiveness of proposed method is verified by simulation and experiment. Stable steady state response with reduced ripple is obtained.*

Key words: *Pulse Width Modulation, Adaptive sliding mode control, Buck Converter, Gain scheduling, Lyapunov Stability*

1. Introduction

In power converters a high premium is placed on the efficiency of power conversion, besides steady state and dynamic performance. The switching property makes the power converters prime candidates for the application of the theory of Variable Structure Systems (VSSs). VSS theory results in a time domain description of switching converters. Switched mode DC-DC converters are nonlinear and time invariant systems. Of these buck converter is a popular choice for various industrial applications.[1] The control of a buck converter over a wide load range and varying voltage is challenging, as the converter dynamics change

significantly between CCM and DCM. Thus, an increased output voltage cannot be reduced swiftly which means that an overshoot of the output voltage has to be avoided or at least limited.

A new proportional–integral-type hyper-plane sliding mode controller (SMC) has been designed for output voltage control of the DC–DC buck/boost converter for its continuous and discontinuous conduction modes of operating conditions. This is based on small signal model and hence is suitable for single operating point. [2]. A robust voltage-mode controller based on Sliding Mode (SM) Control for DC–DC boost converter subject to time varying parameters such as inductors and capacitors is presented. In spite of excellent robustness this simple control structure does not guarantee stable and well-behaved dynamics over a wide operation range.[3] The analysis and design of a hysteretic PWM controller with improved transient response have been proposed for buck converter [4]

Nonlinear control schemes, such as one-cycle control, current-mode control and SM control, have been discussed for DC–DC converters [5]. Among them, SMC has advantages such as simple implementation, insensitive to parameter changes. SMC is a nonlinear controller introduced for controlling VSSs.

ASM control is applied for fixing the switching frequency of SMC. But non-Zero steady-state error cannot be achieved. In spite of achieving constant switching frequency with a sliding surface equivalent control that senses output voltage there are low frequency oscillations on the output waveform [6].

Model Predictive SM controller for boost converter has faster dynamic response with reduced steady state error for operations above the nominal load, but overshoots and ringing in the transient response occurs when operated below the nominal load.[7]. Deepak and Vinodkumar present a robust pulse-width modulation-based sliding-mode controller for a DC-DC boost converter feeding the constant power load in a typical dc microgrid scenario [8]. A unique sliding-mode control law to regulate a bidirectional boost converter with output filter in a seamless manner is proposed where the output voltage of the converter is effectively regulated by means of a proportional–integral controller, while the inner current loop has a sliding-mode current controller. [9]. These approaches are not suitable for a general design approach, as they do not take into account the change of the system dynamics that occurs when changing between CCM and DCM operation. In [10] an alternative control structure, which takes into account the load dependent dynamics to improve the stability of the converter, is proposed. Unfortunately, this solution cannot be used for a conventional buck converter, because it requires a switch antiparallel to the converter diode.

The various approaches regarding gain-scheduling are the classical gain-scheduling approach, more recent Linear Parameter varying (LPV) method [11] and thirdly, fuzzy techniques.

A gain-scheduled controller thus can adjust itself according to the changes in the dynamics of the plant [12]. More recent LPV control synthesis techniques elaborate on this idea using i) parameter-varying Lyapunov functions[13] and ii) scaled small-gain theorems[14]. A LPV model comprises linear, parameter-dependent dynamics [15].

Low voltage circuits are essential to satisfy the demands of single battery operation in portable electronic devices like cellular phones, pagers, laptop computers, Portable device applications, etc. Maximization of battery life, highly power efficient DC-DC converters are desirable factors of battery powered devices. Here load conditions change from high to low power levels ie. from DCM to CCM. The load does not remain in DCM for long periods, rather these devices operate in CCM ie. standby mode for most of the time. Therefore,

improving light-load efficiency of DC-DC converters is crucial for extending battery life.

This paper aims in improving previous controller [16] by modeling system with power losses to improve system performance. A gain scheduled Digital ASM equivalent voltage mode controller working in CCM and DCM that optimizes the dynamic performance during wide

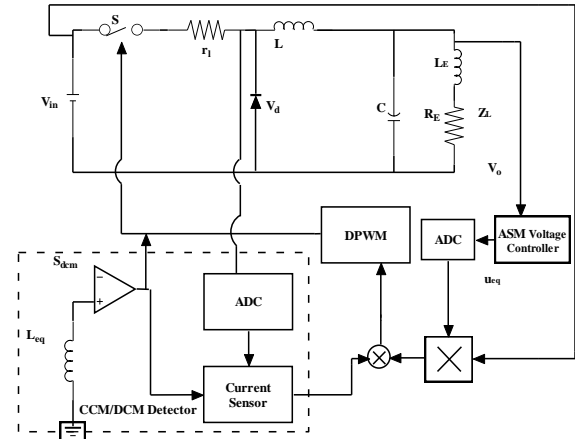


Fig. 1. Proposed Block diagram of Buck Converter

range of load variations for mobile phones is proposed. Converter is modelled with power losses and this model is simplified to incorporate the proposed simple adaptive algorithm. Finally, the proposed controller is applied. This is realized through the incorporation of a gain scheduling scheme into the conventional SM controller. The controller parameters are adaptively varied according to output loading. The work was conducted on a unified topology: buck converter working in both CCM and DCM for mobile phones. This paper aims to present the necessary theoretical background and implementation details that enable the proposed controller to be readily adopted for portable battery applications.

2. Materials and Methods

Switched networks create non-linear time varying problems. Therefore switched network modeling has gained importance to improve the response of system. A modeling procedure for the buck converter case is derived. All the passive elements are assumed to be Linear Time Invariant (LTI) and the switches have only switching loss. The converter is assumed to operate in the CCM and a boundary detector circuit is to be implemented to make it to operate both modes. A new Equivalent SMC

technique to design a controller for mobile batteries is to be used and will be discussed in section 3. Design and implementation of a unified ASM controller for buck converter is to be discussed in section 3.

2.1 Modeling of converter with losses

Design of an SM controller starts with a state-space description of the converter model in terms of the desired control variable, ie. Voltage. The focus of this paper is the application of SM control to converters operating in CCM and DCM. The PWM repeating period is T and the switching frequency $f=1/T$. The duty cycle is represented as a scalar input \bar{u} . The instantaneous values of current and voltage are I_x and V_x for the component X . The input voltage, input current, output voltage and output current are denoted by V_{in} , I_{in} , V_o and I_o respectively. The mobile phone in the circuit is modeled as impedance Z_L .

The state vectors for the converter are

$$X = \begin{bmatrix} x_1 \\ x_2 \end{bmatrix} = \begin{bmatrix} I_l \\ v_o \end{bmatrix}.$$

The state space equation for the buck converter when switch is in ON and OFF condition during CCM and DCM is combined and state space averaged model (1) can be derived as

$$\dot{X} = A_3 X + B_3$$

For buck Converter

$$A_3 = A_1 \bar{u} + A_2 (1 - \bar{u}) = \begin{bmatrix} -\frac{r_{sw} \bar{u} + r_l}{L} & -\frac{1}{L} \\ \frac{1}{C} & -\frac{1}{Z_L C} \end{bmatrix}$$

$$B_3 = B_1 \bar{u} + B_2 (1 - \bar{u}) = \begin{bmatrix} \frac{V_{in} \bar{u} - V_d (1 - \bar{u})}{L} \\ 0 \end{bmatrix} \quad (1)$$

The converter steady state voltage transfer gain M (2) is

$$M = \frac{V_o}{V_{in}} = \frac{\bar{u} - \frac{V_d}{V_{in}} (1 - \bar{u})}{1 + \frac{r_{sw} \bar{u} + r_l}{Z_L}} \quad (2)$$

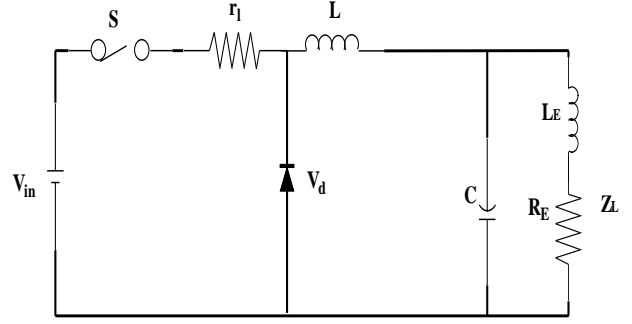


Fig. 2. Simplified model of Buck Converter Equation (2) and (3) shows the impact of practical components on gain term M .

$$A_3 = \begin{bmatrix} -\frac{\bar{u}(r_l + r_{sw})}{L} & \frac{(\bar{u} - 1)}{L} \\ \frac{(1 - \bar{u})}{C} & \frac{\bar{u}}{Z_L C} \end{bmatrix}$$

$$B_3 = \begin{bmatrix} \frac{V_{in}(1 - \bar{u}) - V_d}{L} \\ 0 \end{bmatrix} \quad (3)$$

The lossy terms at normal operating conditions are r_{sw} , r_l and v_d . The representation of practical buck converter is shown in Figure 2.

Steady state voltage transfer gain is shown in (4),

$$M = \frac{(1 - \bar{u}) - \frac{V_d}{V_{in}}}{1 + \frac{r_{sw} \bar{u} + r_l}{Z_L}} \quad (4)$$

The final state space averaged equation with single power loss term r_{loss} is derived as follows.

$$\dot{X} = A X + B \bar{u}$$

For the buck converter the state space averaged model (5) new steady state voltage transfer gain (6) and loss term (7) is shown as follows,

$$A = \begin{bmatrix} -\frac{r_{loss}}{L} & -\frac{1}{L} \\ \frac{1}{C} & -\frac{1}{Z_L C} \end{bmatrix} \quad B = \begin{bmatrix} \frac{V_{in}}{L} \\ 0 \end{bmatrix} \quad (5)$$

$$M_{new} = \frac{v_{out}}{v_{in}} = \frac{Z_L}{Z_L + r_{loss}} \bar{u} \quad (6)$$

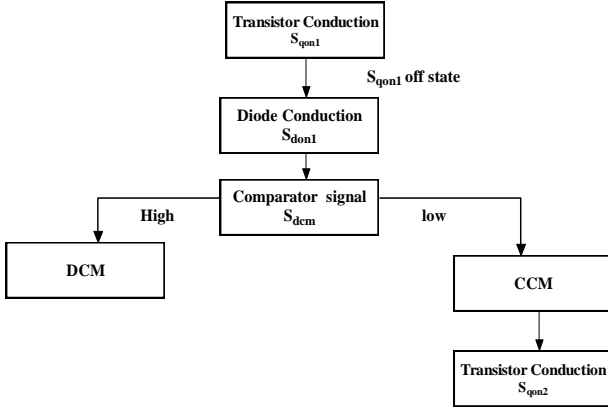


Fig. 3. Control Algorithm for adaptive switching

$$r_{loss} = \frac{V_{in} \bar{u} (r_l + r_{sw} \bar{u}) + Z_L V_d (1 - \bar{u})}{v_{in} \bar{u} - V_d (1 - \bar{u})} \quad (7)$$

The simplified circuit shown in Figure 2 provides same response as that obtained from the basic model of converters. Next design of a unified controller for buck converter is discussed in section 3.

2.2 Adaptive Switching Control for CCM/DCM boundary detections

A Converter operating at the boundary of CCM and DCM is applicable at low power levels. This boundary between CCM (heavy load) and DCM (light load) is necessary because the transfer function between duty cycle d and the output voltage v_o or between input voltage v_{in} and output voltage v_o becomes also dependent on load condition in DCM. Therefore to improve performance the boundary between CCM and DCM has to be predicted [17]. The aim of proposed ASMC is to maintain same sliding coefficients for DCM operation. Detection of zero crossings of the inductor current i_l aids both the high-side and low-side switches to be turned off.

In the CCM/DCM adaptive switching controller proposed in this paper an auxiliary inductor winding and DCM comparator are used to detect zero crossings of inductor current. DCM oscillation period t_{osc} detected by DCM comparator signal S_{dcm} is assumed to remain constant between two consecutive periods. On completion of normal CCM switching period t_s controller waits for transition of S_{dcm} from low signal to high signal. Now the MOSFET turn off time is extended by half of t_{osc} . Therefore next

cycle of DCM ends at a point when i_l is zero. This facilitates the calculation of current sensing factor k_{sense} (8). The discontinuous conduction interval t_{dcm} is measured and k_{sense} is calculated as

$$k_{sense} = 1 - \frac{t_{dcm}}{t_s} \quad (8)$$

The illustration of adaptive switching controller is shown in Figure 3.

Using the above algorithm the adaptive CCM/DCM control law is shown in (9).

$$e_i[n] = t_{sw} \cdot i_{ref} - (t_{sw} - t_{dcm}) i_{lsense} \quad (9)$$

where t_{sw} is adaptive switching period. From the control chart we can conclude that the DCM comparator output decides the switching between high level and low level state.

3. Proposed Digital ASM Controller

Buck converters are time variable and a nonlinear switching circuit which possesses variable structure features. In the following section, design of control equations for the proposed method to improve the dynamic response is outlined. A new variation of Sliding mode control of PWM buck converter is proposed. The detailed procedure for designing unified Digital ASM controller for buck converters in CCM and DCM operation is discussed in the following.

3.1 Sliding Mode Control Approach

Design of robust controller is made possible using SMC methodology. The two advantages of this approach are: The dynamic behaviour of the system is decided by the particular value of reference chosen for the switching function. Therefore closed-loop response is not affected by any system uncertainties. The two step design approach is as follows:

1. Design of a sliding motion switching function to satisfy the design specifications.
2. Selection of a control law to make the switching function feasible to the system state. Traditional SMC employs a sliding manifold(10) as

$$\sigma(x, t) = SX + \varphi = 0 \quad (10)$$

where $S=[S_1, S_2, S_3, \dots, S_N]$ and ϕ is the reference value obtained from state space equation. If the representing point (RP) slides on the sliding surface $\sigma(x,t)=0$ the system is said to be in sliding mode. The existence condition (11) is

$$\lim_{\sigma \rightarrow 0} \sigma \cdot \frac{d\sigma}{dt} < 0 \quad (11)$$

The sufficient condition for the system to reach the sliding surface is if the RP is initially in one subsystem it will hit the sliding surface in spite of its initial position in finite time. Considering the system operation over the sliding region the sliding function satisfies the condition shown in (12).

$$\sigma(x,t) = 0, \frac{d\sigma(x,t)}{dt} = 0 \quad (12)$$

$$\dot{\sigma}(x,t) = S \dot{X}$$

Using equations (5) (10) and (12) we get the reaching condition for sliding mode control (13).

$$S\dot{X} + \dot{\phi} = SA(x,t) + SB(x,t)d_{eq} + \dot{\phi} = 0 \quad (13)$$

where d_{eq} is duty cycle input. The expression for equivalent control (14) is

$$d_{eq} = -(SB)^{-1}SA(x,t) \quad (14)$$

By substituting (17) into (1) the state space equation derived is

$$\dot{X} = [I - B(SB)^{-1}S]A(x,t) \quad (15)$$

The above equation represents the system dynamics under SMC (15).

3.2 Equivalent Controller using SMC

An equivalent translation of SM control law is adopted for PWM based ASMC. The equivalent control signal $\overline{u_{eq}}$, a smooth function of discrete input function \overline{u} is formulated using the invariance condition. The final duty ratio of pulse width modulator is derived from equivalent control function. The switching frequency is made constant using the new calculated duty cycle. Here a reference term is added to traditional sliding manifold (10) to form a new sliding surface (16) proposed is

where, modified $\phi = \int_0^t (v_o - v_r) dt$ and

$$S = [\alpha, \beta] \quad (16)$$

For buck converter:

The new existence condition for the changed sliding surface for the simplified model is given in (17)

$$\begin{aligned} \sigma(x,t)_{u=1} &= \alpha \left(\frac{r_{loss} + Z_L}{Z_L} V_r + V_{in} \right) > 0 \\ \sigma(x,t)_{u=0} &= \alpha \left(-\frac{r_{loss} + Z_L}{Z_L} V_r - V_d \right) < 0 \end{aligned} \quad (17)$$

The modified existence condition (18) is

$$\begin{aligned} \frac{Z_L V_{in}}{r_{loss} + R_L} - V_r &> 0 \\ -V_r &< 0 \end{aligned} \quad (18)$$

The reaching and existence conditions of both converters are same for original and simplified model. The unified sliding equivalent control becomes as shown in (19).

$$\overline{u_{eq}} = -[SB]^{-1}[SA(x,t) + (V_o - V_r)] \quad (19)$$

Now the choice of switching frequency is according to open loop model of the converters. The proposed unified sliding mode equivalent controller expression (20) for buck converter is

$$\overline{u_{eq}} = \frac{\frac{\alpha}{L}(r_{loss}x_1 + x_2) - \frac{\beta}{C}\left(x_1 - \frac{x_2}{Z_L}\right) + (V_r - x_2)}{\frac{(\alpha V_{in})}{L}} \quad (20)$$

From the equivalent controller expressions (20) it is inferred that the numerator terms are same as that of PID controller. The simplified controller expression is shown in (21)

$$\overline{u_{eq}} = \frac{\frac{\alpha}{L}(r_{loss}x_1 + x_2) - \frac{\beta}{C}i_c + (V_r - x_2)}{\frac{(\alpha V_{in})}{L}} \quad (21)$$

The controller expression (20) is called non-adaptive controllers. In addition to variation in input voltage, load impedance variations has to be considered to make the system adaptive and to get a better dynamic response. The closed loop system is obtained by substituting $\overline{u_{eq}}$ in (5). The closed loop model is given in (22)

$$\dot{X} = \begin{bmatrix} -\frac{\beta}{\alpha C} & \frac{\beta - Z_L C}{\alpha Z_L C} \\ \frac{1}{C} & -\frac{1}{Z_L C} \end{bmatrix} X + \begin{bmatrix} \frac{1}{\alpha} \\ 0 \end{bmatrix} V_r \quad (22)$$

3.3 Modelling of ASM Controller

The equivalent SMC proposed operates under the assumption that the losses are known. So to estimate r_{loss} adaptive law (23) is designed by introducing a new state variable x_3 .

$$\dot{x}_3 = \gamma \mathcal{W}_r (V_r - x_2) \quad (23)$$

where γ is adaptive coefficient which determines the switching frequency of controller. The selection of γ is made in order to achieve fast response. The optimal controller in (21) after introducing adaptive coefficient becomes as shown in (24).

$$u_{eq} = \frac{\frac{\alpha}{L}(x_3 x_1 + x_2) - \frac{\beta}{C} i_c + (V_r - x_2)}{\frac{(\alpha V_{in})}{L}} \quad (24)$$

The closed loop state space averaged equation obtained is as follows(25).

$$\dot{X} = \begin{bmatrix} -\frac{\beta}{\alpha LC} & \frac{\beta - Z_L C}{\alpha Z_L C} & \frac{V_r}{Z_L} \\ \frac{1}{C} & -\frac{1}{Z_L C} & 0 \\ 0 & -\gamma V_r & 0 \end{bmatrix} X + \begin{bmatrix} \frac{1}{\alpha} \\ 0 \\ \gamma V_r \end{bmatrix} v_r \quad (25)$$

In this paper discretization of ASMVC designed in the continuous-time domain is implemented. In simulations, systems are usually discretized using the Euler method, while a zero-order holder (ZOH) is used in practical implementation of the ASMVC. The resulting dynamics can be written as $\dot{X} = Ax + Bu_{eq}$

The switching logic discussed in section 2.2 helps the state trajectory to follow the desired path. The next step in controller design is stability analysis.

3.4 Stability Analysis using Lyapunov stability criterion

To verify the proposed controller analytically global stability analysis is done using system equations derived in section 2. The Second Lyapunov Method was found on the so called energetic approach to stability analysis. In this method evolution of energy of a dynamic system over time for any positive definite function is studied. The dynamic system with decreasing energetic function along any trajectory has a stability property and the decreasing energetic function is called Lyapunov function

To prove stability of a system a continuously differentiable positive definite function $V(x)$ is defined. The classical condition of Lyapunov function (26) can be written as

$$\dot{V}(x) = V^T(x)V(x), f(t, \infty) < 0 \quad (26)$$

AS dv/dx is always negative, system is said to be asymptotically stable if apparently V decreases continuously, and the state must end up in the origin of the state space. To develop these concepts, from the sign of V and V' :

For negative dv/dx system is globally asymptotic, it is unstable if dv/dx is positive definite or semi definite and if dv/dx is indefinite then it is not possible to decide about stability. According to statement of Lyapunov's criterion (27)

$$V = \frac{1}{2} S^2 > 0 \quad \text{and} \quad \dot{V} = S\dot{S} \quad (27)$$

if $S \neq 0$. Now using above in buck converter system equations the stability criterion for SMC (28) is

$$V = \frac{1}{2} (V_o - V_r)^2 \quad (28)$$

Time derivative of equation (28) is given in (29)

$$\dot{V} = (V_o - V_r) \frac{1}{C} V \left[\frac{V_s}{V_o} i_{ref} - \frac{V_o}{Z_L} \right] \quad (29)$$

$$\begin{aligned} &= (V_o - V_r) \frac{1}{C} \left[\frac{V_r^2}{V_o Z_L} - \frac{V_o}{Z_L} \right] \\ &= -(V_o - V_r) \frac{1}{C V_o} [V_o^2 - V_r^2] \\ &= -(V_o - V_r) \frac{1}{C V_o} (V_o - V_r)^2 (V_o + V_r) \end{aligned} \quad (30)$$

From the inequality (30) we can conclude that time derivative of V is negative semi definite for $V_{in} > 0$ and the system is globally stable.

To check for local stability, it is sufficient to prove that V be locally positive definite and derivative of V be locally negative definite. With this definition, the characterizations of stability and asymptotic stability carry through to the local case. From (29) and (30) both local and global stability is inferred. The closed loop representation for buck converter is simulated and experimentally validated. The results are discussed in the following section.

4. Simulation Results and Discussions

The dynamic response of the ASM voltage controller for battery operated mobile phones is

obtained by simulating a 150mW buck converter for a load variation from 25 mΩ to 100 mΩ. is performed using MATALB/ Simulink software.

Table 1 Buck Converter Specification

Description	Parameter	Nominal Value
Input Voltage	V_i	6 V
Capcitance	C	47μF
Inductance	L	8.2μH
Switching frequency	f_{sw}	200KHz
Min. Load Impedance	Z_{Lmin}	25mΩ
Max. Load Impedance	Z_{Lmax}	100mΩ
Output Voltage	V_o	2 V

4.1 Simulation results

Table 1 shows the specifications for buck converter .The effect of ASMVC on the output voltage and inductor current is observed for the following conditions in this section.

- Transient region (turn on region),
- Under line and load variations (disturbances)

By examining Figure 4 it could be seen that the maximum overshoot of output voltage for SM controlled buck converter is 3.5 V, while the overshoot of inductor current is 100 mA . The maximum overshoot should not exceed 10% of the steady state value according to standards, but the maximum overshoot of the output voltage and inductor current is higher than 10%. The analysis of line and load variations reveals the following:

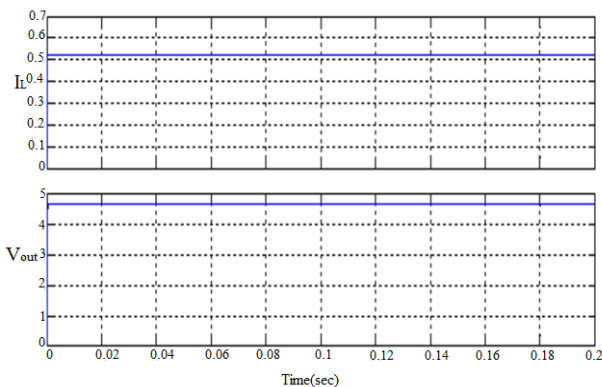


Fig. 4. Output voltage and Inductor current of SMVC Buck Converter

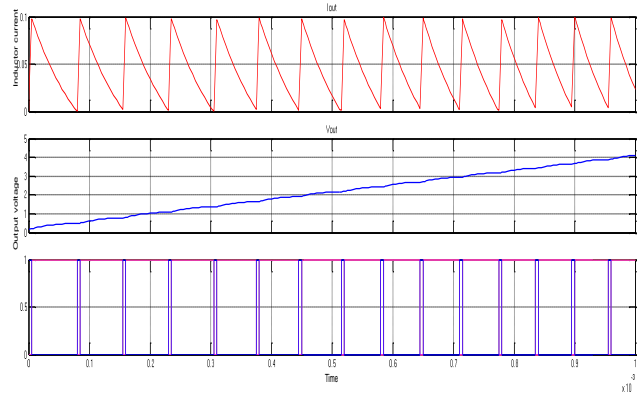


Fig. 5. Output voltage and Inductor current of ASMVC Buck Converter

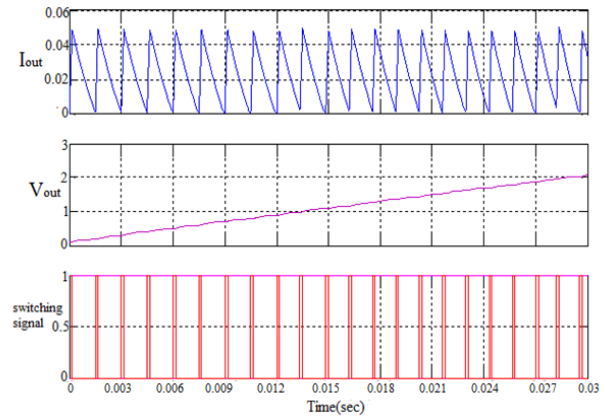


Fig. 6. Output voltage and Inductor current of Digital ASMVC Buck Converter

The effect of line variation was analyzed by applying a step change in the input voltage from 6 volt to 10 volt. It could be inferred from Figure 4 that SMC will force the output voltage and inductor current to stay in a stable mode with infinitesimal change in the output voltage. The load was changed from 25 mΩ to 100 mΩ and figure 4, 5 and 6 shows the simulated waveforms for buck converter using SMC, ASMVC, and Digital ASMVC.

Load changes are made linearly from 25mΩ to 100 mΩ. As load value increases the converter transfers its operation from CCM to DCM. The converter operates in CCM for changes from 15 mΩ to 45 mΩ .DCM starts at 50 mΩ during which output ripple voltage increases .The inductor current changes from CCM to DCM as load value changes from nominal load.

From the startup transient response of the buck converter using SMC variation of the input voltage from 6 V to 10 V is analyzed. The settling time is 0.07 sec at the nominal input voltage of 5V. The output profile is from 4 to 4.5 V. The settling time of the buck converter using

SMC is 0.05 sec for load changes from 25 mΩ to 100mΩ at nominal input voltage.

The buck converter output waveforms for same voltage changes using ASMVC are observed. The settling time was about 0.0291 sec at the nominal input voltage of 6V. As the input voltage increases from 6 V to 10 V, the settling time decreases. The voltage profile changes from 3.5 to 4.1 V. For load changes from 25 mΩ to 100mΩ. The output voltage of the buck converter using ASMC settles at about 0.02 sec.

A comparison between the PWM based sliding mode controller and ASM controllers for DC-DC buck converter is done. Unified Controller working in CCM and DCM for DC-DC converters is evaluated in simulation under the input voltage and load variation. The comparison between SM controller and ASM Controller is given in Table 2.

Table 2 Comparison of SM controller with ASM Controller

Type	Settling time ms	Rise time ms	Overshoot percentage %	Peak voltage V	Ripple voltage mV
SM controller	0.39	0.219	26.3	4.9	1.9
ASM controller	0.015	0.120	21	4.1	1.15
Digital ASM Controller	0.005	0.021	5	2	0.245

4.2 Prototype model of Converter

The circuit representation of the prototype model is shown in figure 7. The working is as follows. The difference of output voltage and reference voltage is fetched using EL2244/EL. The difference is integrated using opamp EL2244. After various synthesis stages the comparator LM111 output is fed to drive circuit. The switching signal is converted to digital. Detecting CCM/DCM modification is achieved by comparator LM111. The output signal is fed to ADC 7890. Further the output signal is applied to gate source of switching device IRF530. The buck converter is experimentally validated by means of the hardware model shown in figure 8.

The simulated and experimental results for digital ASMVC buck converter for input voltage of 6V with linear load impedance of 100mΩ is shown in figure 6 and 9. An output voltage of 2 V is achieved in 0.03 ms. The simulation results for operation of buck converter during a voltage step from 6 to 10 V is shown in figure 10a.

Table 3 Comparison of simulated model with experimental model for buck converter

Type	Settling time ms	Rise time ms	Overshoot percentage %	Peak voltage V	Ripple voltage mV
Simulated model	0.21	0.0212	1	2.1	0.245
Experimental model	0.31	0.02	1	2	0.299

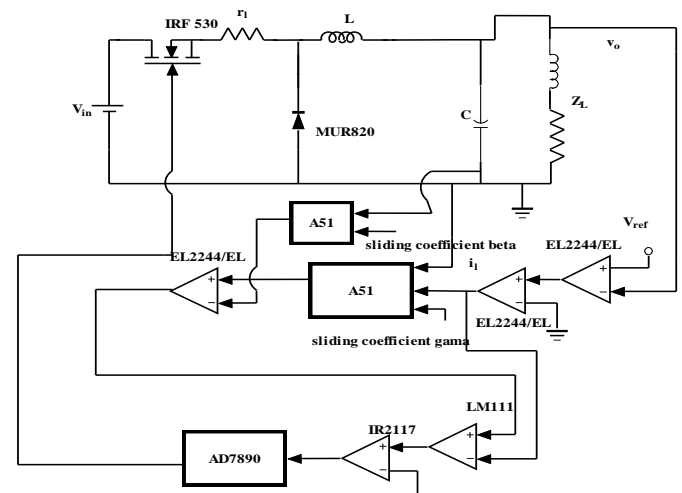


Fig. 7. Prototype implementation of ASM controller



Fig. 8. Experimental model of ASM controller

The reference voltage step is low-pass filtered by the EL2244 opamp resulting in a smooth voltage transient. The converter operates in DCM before the transient as seen from the discontinuous inductor current. It is shown that during the transient, the converter leaves DCM and enters CCM, whereas the output voltage remains unaffected from this operation mode change and output voltage maintains at 2.4 V. After the transient, the buck converter operates in CCM. This experimental results shown in figure 10 b demonstrates that the proposed ASM controller enables a smooth transition between both operation modes of the converter and thus allows operating the buck converter within a wide load range.

The prototype model responds the same as simulation model for line and load variations. Comparisons of simulated and experimental results are tabulated in Table 3 and is represented graphically in figure 11 and 12. The efficiency of the circuit is evaluated to check for power losses. The results show an efficiency of 95.5%. PWM based adaptive sliding mode controller exhibits better performance under input voltages changes.

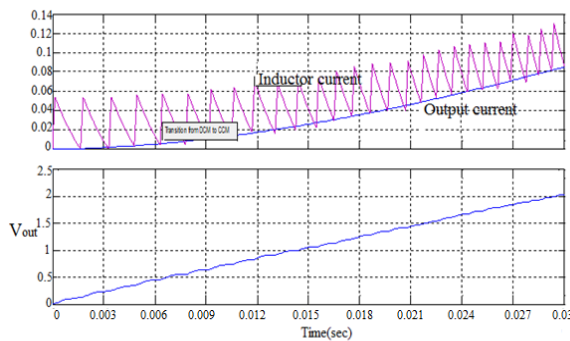


Fig. 9 Gate pulse and output voltage for Digitally controlled ASMVC

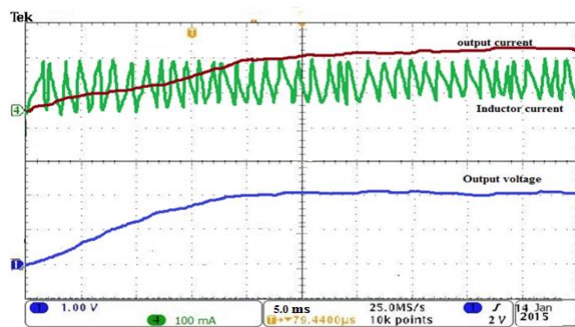


Fig. 10a Output and input voltage for step changes of 6v to 10 V buck converter with input voltage of 6 V for Digital ASMVC buck converter

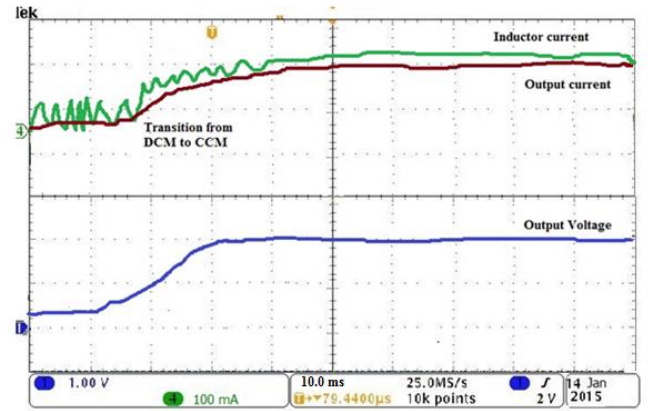


Fig. 10b Output and input voltage for step changes of 6v to 10 V

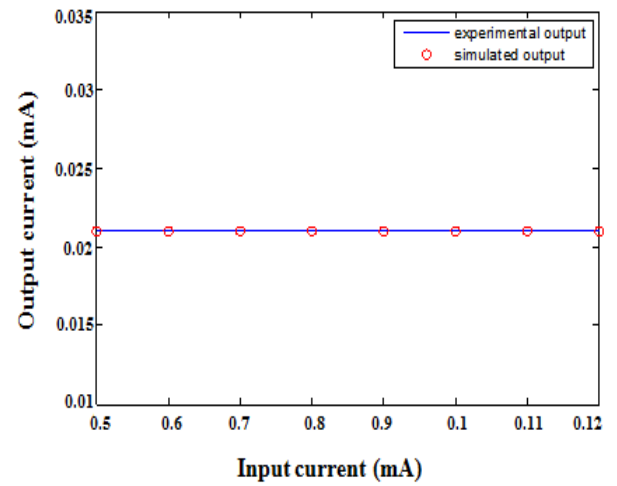


Fig. 11 Comparison of Simulated experimental output voltage for Digital ASMVC buck converter

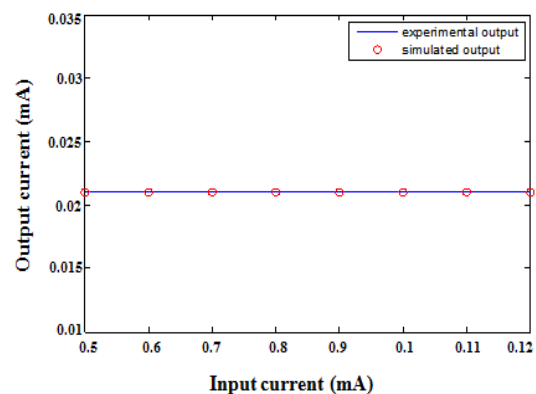


Fig. 12 Comparison of Simulated experimental output current

5. Conclusion

A unified Digital ASM voltage controller for DC-DC buck converter working in CCM and

DCM has been proposed and verified by computer simulation. The designed controller acts as input for mobile phones. The mathematical modeling and computer simulated verification of the PWM based ASMC have been presented. A gain scheduling scheme which monitors the output voltage and load current to vary the sliding line of the system is verified. The adaptive SM controlled converter has faster transient response with reduced steady state error above the nominal load and ripple is minimized when operated below the nominal load. The output voltage and inductor current returns to steady state after line and load variation. Thus the proposed converter system acquires the feature of achieving a stable steady-state response and swift transient response under varying operating points. In future the proposed unified controller shall be tested for all converters.

ACKNOWLEDGMENT

The authors are grateful to the management and principal of ULTRA college of Engineering and Technology for Women for providing all facilities for their research work.

References

1. Vander Broeck, C. H. , De Doncker, R. W., Richter, S. A., Von Bloh, J. (2014): Discrete time modeling, implementation and design of current controllers. *Proc. IEEE IEEE Energy Conversion Congress and Exposition ECCE, Pittsburgh*, 540–547.
2. Mahdi Salimi, Jafar Soltani, Adel Zakipour : Hyper-plane sliding mode control of the DC–DC buck/boost converter in continuous and discontinuous conduction modes of operation. In: IET Power Electronics, No.8,2015,p.1473 – 1482.
3. Hattab A., Chenafa M., Daaou B., Mansouri A., Bouhamida M.: A High Order Sliding Mode Control for Autonomous Underwater Vehicle (AUV). In: Journal of Electrical Engineering, No.2,2015,p.131-138
4. Jianfeng Dai, Jinbin Zhao , Yongxiao Liu , Keqing Qu ,(2013) : PWM hysteresis control with inductor current for buck converter, Renewable Power Generation Conference (RPG 2013), 2nd IET , Beijing ,September 2013,1-4.
5. Luis Martinez Salmero, German Garcia , Marcos Orellana : Analysis and design of a Sliding mode strategy for start up control and voltage regulation in a buck converter. In: IET Power Electronics, No.6,2013,p.52-59.
6. Liquan Shen , Dylan Dah-Chuan Lu , Chengwei Li : Adaptive sliding mode control method for DC–DC Converters. In: IET Power Electronics, No.8,2015,p.1723– 1732.
7. Karamanakos ,P., Geyer T., Manias S.: Direct Voltage Control of DC–DC Boost Converters Using Enumeration- Based Model Predictive Control. In: IEEE Transactions on Power Electronics No.29,2013,p.968 – 978.
8. Deepak Fulwani, Vinod Kumar : Robust Sliding Mode control of DC-DC boost Converter feeding constant power load. In: IET Power Electronics, No.8,2015,p.1230 – 1237.
9. Laura Albiol-Tendillo , Enric Vidal-Idiarte, Javier Maixe-Altes : Seamless Sliding Mode control for bidirectional boost converter with output filter for electric vehicle applications. In: IET Power Electronics, No.8,2015,P. 1808 – 1816.
10. Zhao, Y., Qiao, W., Ha, D. : A sliding-mode duty-ratio controller for DC/DC buck converters with constant power loads. In: IEEE Transaction on Industrial Applications, No.50 2014,p.1448–1458.
11. Olalla, C., Leyva, R., Queinnec, I., Maksimovic, D. : Robust Gain-Scheduled Control of Switched-Mode DC–DC Converters. In: IEEE Transactions on Power Electronics, No. 27, 2012,p.3006-3019.
12. Engelen, K., De Breucker, S. ,Tant, P., Driesen, J. : Gain scheduling control of a bidirectional DC-DC converter with large dead-time. In: IET Power Electronics, No.7,2014,p. 480 – 488.
13. Su, J.-T., Liu, C.-W : Gain scheduling control scheme for improved transient response of DC/DC converters. In: IET Power Electronics, No.5,2012,p.678 – 692.
14. Rodriguez, E.J.A. , Rosas, R.A.P.: Design of a Gain Scheduling Control Based on Linear Matrix Inequalities for a Dynamic System. In: Latin America Transactions, IEEE, No.10 ,2012,p.1459 – 1465.
15. Pankaj Swarnkara, Shailendra Kumar Jaina , R.K Nema : Adaptive Control Schemes for Improving the Control System Dynamics: A Review, In: IETE Technical Review, No. 31, 2014,p.17-33.

16. Muhammad Asif , Muhammad Junaid Khan ,Ning Cai : Adaptive sliding mode dynamic controller with integrator in the loop for nonholonomic wheeled mobile robot trajectory tracking.In: International Journal of Control,No.87, 2014,p.964-975.
17. Vesely,V., Ilka,A.: Gain-scheduled PID controller design.In: Journal of Process Control,No. 23, 2013,p.1141–1148 .

Nomenclature

<i>Symbol</i>	<i>Description</i>	<i>Symbol</i>	<i>Description</i>
V_{in}	Input Voltage	t_s	CCM Switching Period
V_o	Output Voltage	γ	Adaptive Coefficient
d	Duty Ratio	i_{ref}	Reference Current
i_o	Output Current	u_{eq}	Equivalent Control Signal
k_{sense}	Feedforward Path Gain	\overline{u}	Discontinuous Input Function
i_c	Capacitor Current	x_1, x_2, x_3	State Variables
α, β	Sliding Coefficient	V_r	Reference Voltage
i_l	Inductor Current	L	Inductor
s_{dcm}	DCM Amplifier Signal	C	Capacitor
t_{dcm}	Discontinuous Conduction Interval	L_E	Load Inductance
$V(x)$	Lyapunov Function	R_E	Load Resistance
t_{osc}	Dcm Oscillation Period	Z_L	Load Impedance